

## Quantum Dot Quantum Computing Program

### PROGRAM MANAGER

Prof Halina Rubinsztein-Dunlop – UQ

### ATOMIC MANIPULATION AND IMAGING RESEARCHERS

**Students** Mr Mike Dalley (MSc)  
**Staff** Dr Mark Fernée, Dr Bradley Littleton

### COLLABORATING CENTRE RESEARCHERS

**University of Queensland, Australia**  
Prof Gerard Milburn

### OTHER COLLABORATORS

**University of Melbourne, Australia**  
Prof Paul Mulvaney  
**University of Queensland, Australia**  
Dr Warwick Bowen  
**University of Queensland, Australia**  
Dr Taras Plakhotnik

### PROGRAM DESCRIPTION

The aim of this program is to develop a single photon source suitable for all-optical quantum computer technologies based on precise electrical control of a cavity quantum electrodynamical interaction between a single photon and a quantum dot (or other suitable “artificial atom”). The program is focussed on the use of high quality fused silica micro-cavities and associated fibre-based output coupling. Nanocrystal quantum dots are suitable for use with fused silica microcavities allowing strong quantum electrodynamical interactions between the cavity and nanocrystal, which can be used to carefully prepare and collect single photons with high efficiency. The various steps that are being undertaken are identification and characterisation of a quantum dot suitable for use in a single photon source, demonstration of the basic operational principles (such as an electric field induced Stark shift), manufacture and characterisation of sufficiently small fused silica microcavities and the demonstration and characterisation of an electrically controlled single photon source.

### 1. Spectroscopic thermometry

Effective thermometry of single nanocrystals mounted on crystal quartz substrate, which is clamped to a liquid helium-cooled cold finger, has been developed. Standard thermometry using a calibrated resistor was found to be inaccurate due to the distance between the sensor and the sample. Furthermore, any standard sensor would be unable to account for the effects of the optical pumping process, which is known to heat the nanocrystal. In order to overcome this difficulty, we fit a numerical model to a series of temperature dependent spectra, which constrains the actual nanocrystal temperature to within 4 K of the sensor-measured temperature.

With accurate thermometry, we were able to determine the acoustic phonon lifetime in the nanocrystals as of the order of 6.5 ps, which

is far faster than the exciton lifetime (Figure 1). This rapid phonon relaxation lifetime indicates that the nanocrystals reach thermal equilibrium before emitting a photon. Therefore a small phonon coupling is necessary to prevent significant dephasing of the exciton transition, which is a requirement of a good single photon source. We have found this to be the case in single CdSe based nanocrystals.

### 2. Sources of spectral instability

Single CdSe based nanocrystals are observed to exhibit significant spectral instability at the time scale common to our experiments (seconds to minutes). We sought to understand this instability and to characterize the time scale over which it occurs. Two different approaches were used: High resolution Fabry-Perot spectroscopy and a statistical search for correlations.

Use of the high resolution Fabry-Perot spectrometer (Figure 2) was problematic at the long 30 s exposure times required for this experiment. However, we were able to detect some throughput from approximately 10% of the nanocrystals studied. A throughput contrast method was employed to limit the underlying line width to less than 20  $\mu\text{eV}$ . Although not

the narrowest reported linewidth for a single nanocrystal, this result is significant because of the time scale. It shows that the underlying linewidth of a single nanocrystal on a 30 s time scale is approximately that determined by an asymptotic limit reached at a millisecond time scale. This suggests that the spectral instability we observe only manifests itself at long time scales from seconds to minutes.

We quantified the above result using a statistical treatment of the random fluctuations. When analysing long time series of spectral peak positions, we find that for nanocrystals of a certain size, the peak fluctuations are not completely random, but contain significant correlations (Figure 3). A theory of Poissonian noise derived from fluctuating two-state systems indicates that significant correlations can arise in a time series only for a fluctuation rate (during a single spectral acquisition period),  $N < 1$ . We were able to confirm this prediction with the data. Therefore, using this narrow range for the fluctuation rate,  $N$ , we determined that the single nanocrystal spectral stability was of the order of  $10^4$  emitted photons per single spectral jump, indicating that the process causing the spectral instability is only weakly coupled to the exciton transition. Such a weakly coupled process is not a major obstacle for the use of these nanocrystals in a single photon source.

Another important outcome of this work is that the dominant spectral instability is also identified as a single physical process. This rules out random environmental charge motion and points to a surface ligand instability as cause. It is most likely that the process corresponds to the photo-induced removal and re-attachment of single ligand molecules from the surface of the nanocrystal. This identification should facilitate means of improving the nanocrystal synthesis in order to minimise or remove this instability entirely.

Luminescence intermittency, or blinking, is another type of nanocrystal instability. This phenomenon is still not well understood in these materials and can be detrimental to our application. A recent development of non-blinking nanocrystals promises that this instability can be overcome. However, we have managed to identify a new and potentially important process resulting in intermittency. Using a specific CdSe/CdS core/shell nanocrystal, that restricts the hole to the core while only weakly confining

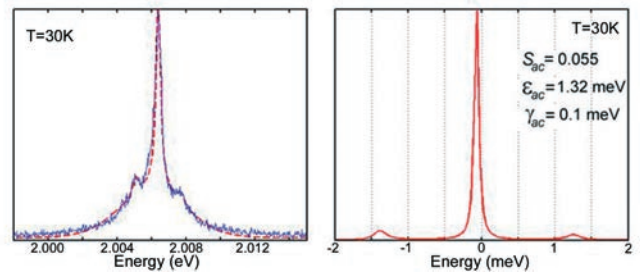


**FIGURE 1**  
a) Emission spectrum from a single CdSe nanocrystal at 30 K exhibiting discrete acoustic phonon sidebands. A fit using a quantum mechanical model is also shown (red). b) The simulation result including the parameters used in the fit. Rapid acoustic phonon relaxation is indicated.

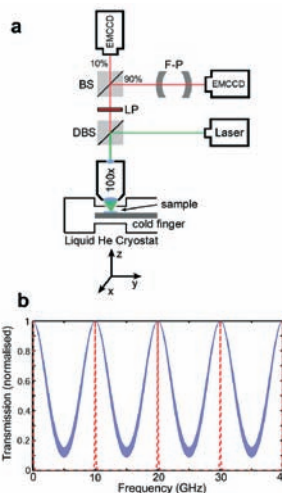


**FIGURE 2**  
a) Schematic of the high resolution Fabry-Perot interferometer. b) Simulated output from the Fabry-Perot interferometer using parameters determined from our data, in the absence of spectral instability.

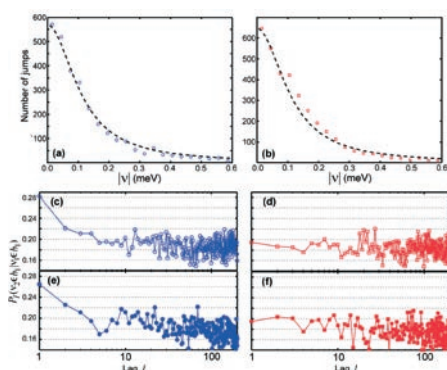


**FIGURE 3**

(a) Histogram of spectral jump magnitudes (blue circles – bin width 30  $\mu\text{eV}$ ) obtained from a series of 3163 individual 1 second spectra from a single 6 nm core diameter NC. (b) Histogram of spectral jump magnitudes (red squares – bin width 30  $\mu\text{eV}$ ) obtained from a series of 3552 individual 1 second spectra from a single 10 nm core diameter NC. The dashed lines represent Lorentzian fits to the data. (c–f) Conditional probability that a second spectral jump resides in the first spectral bin,  $l$  jumps after finding the first jump resides in this bin ( $P(v \in b_l | v \in b_1)$ ), where  $b_i: 0 \leq v < 60 \mu\text{eV}$ ). (c) Single 6 nm core diameter NC shown in (a) (blue open circles). (d) Single 10 nm core diameter NC shown in (b) (red open squares). (e) Ensemble of 20 single 6 nm NCs comprising 2945 jumps. (f) Ensemble of 21 single 10 nm NCs comprising 2339 jumps. 60  $\mu\text{eV}$  bin widths are used throughout.

the electron, we revealed a novel three-state blinking process (Figure 4). This new process includes an intermediate state that mediates the complete luminescence “off” step. The “off” state was determined to correspond to a surface-trapped electron, which results in an efficient non-radiative relaxation pathway. However, the intermediate state also exhibited a somewhat less efficient non-radiative pathway. This state was identified as a state of imperfect surface passivation, where the presence of just a single electron trap at the surface enables an efficient exciton relaxation pathway. This new relaxation pathway is opened by the removal of just a single surface molecule. An efficient surface-related exciton relaxation pathway requires improvements in surface passivation to overcome. However, it is yet to be established whether this mechanism operates at cryogenic temperatures, where there is little thermal energy to assist the process.

### 3. Long spin lifetimes

The luminescence from single CdSe/CdZnS core/graded shell materials (which we are investigating) usually show spectral doublets (Figure 5). We have shown the doublets to be emission from both the bright and dark exciton fine structure states. In contrast, all previous reports of single nanocrystal luminescence show only single spectral lines attributed to dark exciton luminescence. The observation of spectral doublets thus represents a significant improvement in the photo-physical properties of these materials, as it indicates that an efficient spin relaxation pathway can be controlled using synthetic procedures. We have quantified the spin relaxation rate in different single nanocrystals using thermal redistribution of population in conjunction with a rate equation analysis (Figure 6). Spin lifetimes longer the bright exciton lifetime are found, which are now comparable to those found in self-assembled quantum dots comprising state-of-the-art single photon sources. Our results also indicate that this spin relaxation channel can be manipulated using different surface treatments. Ultimately the complete suppression of dark state emission would be desirable in these materials.

### 4. Stable trion emission

The detection of spectroscopic fine structure has enabled us to identify the charge state of

a single nanocrystal. A charged state is noticeable by the absence of spectral fine structure. We have found many examples of doublet and triplet fine structure emission that switches to singlet emission. Using polarisation-resolved detection we were able to show that the low energy state of a doublet switches off in the transition to the singlet, while the polarisation of the upper state is maintained in the singlet emission (Figure 7). Furthermore, the spectral red shift of 5 meV identifies the singlet emission state as a negatively charged,  $X^{(-)}$  trion state. This then indicates that the hole becomes trapped (most probably in a residual core/shell interface defect state), suggesting single defect doping as a means to enhance and further stabilize the trion state in colloidal nanocrystals.

The detection of a stable trion state is significant for a single photon source, as the lack of surrounding fine structure states can significantly reduce interference and scattering from the nearby states, which is a common source of decoherence. The trion state is also brighter than the neutral state at cryogenic temperatures, as the transition is optically allowed (as opposed to the dark state emission which has a long microsecond lifetime). Furthermore, the trion state can be used in coherent pumping schemes to produce photons with excellent non-classical interference properties. The state also has a well defined spin, enabling spin storage and manipulation suitable for quantum memories and gates.

### 5. Micro-cavity fabrication and characterization

High quality micro-toroids along with adiabatic output couplers are being supplied through a collaboration with Dr Warwick Bowen. These cavities represent the state-of-the-art and are being tailored to our single photon source application using material properties that we have established. Furthermore, toroidal micro-cavities are superior to micro-spheres for our application due to their close proximity to a silicon substrate, which can facilitate efficient cooling of the cavity system to cryogenic temperatures. Cryogenic studies of these cavities will soon be under way.

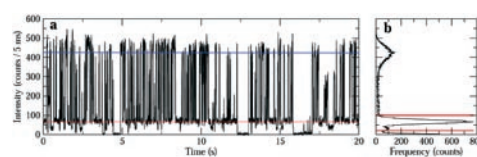


**FIGURE 4**

(a) Time series if emission level for a single CdSe/CdS core/shell nanocrystal at room temperature in a standard atmosphere. The horizontal red line indicates an intermediate emission level attributed to a state of imperfect surface passivation following desorption of a single molecule. (b) A histogram of emission levels indicating all three states of the system.

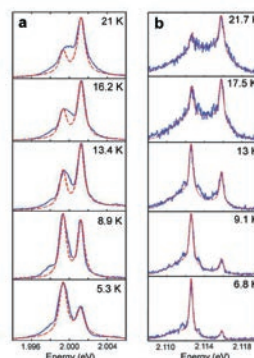


**FIGURE 5**

(a) A series of spectral doublets obtained from the same single nanocrystal (10 nm core diameter) at different temperatures. (b) A series of spectral doublets obtained from the same single nanocrystal (6 nm core diameter) at different temperatures.

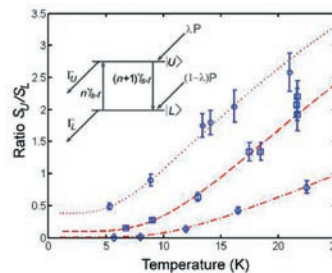


**FIGURE 6**

Temperature dependence of the spectral fine structure for three single nanocrystals. Each data set is fit to a rate equation model indicated in the inset.

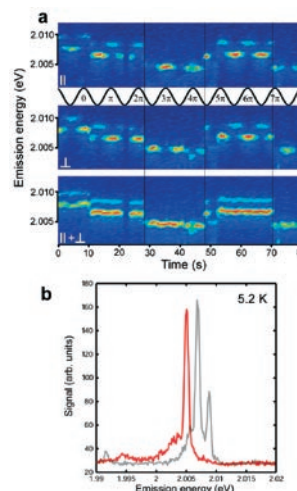


**FIGURE 7**

Doublet to singlet switching. (a) Polarisation resolved spectra of a single nanocrystal (10 nm core diameter) obtained at 5.2 K. Two orthogonal polarisation projections are shown along with the sum of the two projections. The phase angles correspond to the polarisation projection obtained by rotating a half wave plate. Vertical lines indicate switching transitions. (b) Comparison of the singlet and doublet spectra obtained in (a). The singlet is red shifted approximately 5 meV from the high energy peak of the doublet, consistent with the  $X^{(-)}$  charged exciton state.